Received: 16 July 2021 | Revised: 7 September 2021 | Accepted: 20 September 2021
DOI: 10.1002/eco.2363

RESEARCH ARTICLE

WILEY

Behavioural response of brown trout (*Salmo trutta*) to total dissolved gas supersaturation in a regulated river

Robert J. Lennox[1] | **Kirstine Thiemer**[2,3] | **Knut Wiik Vollset**[1] | **Ulrich Pulg**[1] | **Sebastian Stranzl**[1] | **Cecilie Iden Nilsen**[1] | **Thrond Oddvar Haugen**[2] | **Gaute Velle**[1,4]

[1]Laboratory for Freshwater Ecology and Inland Fisheries, NORCE Norwegian Research Centre, Bergen, Norway

[2]Department of Ecology and Natural Resource Management, Norwegian University of Life Sciences, Aas, Norway

[3]Section for Freshwater Ecology, Norwegian Institute for Water Research, Oslo, Norway

[4]Department of Biological Sciences, University of Bergen, Bergen, Norway

Correspondence
Robert J. Lennox, Laboratory for Freshwater Ecology and Inland Fisheries, NORCE Norwegian Research Centre, Nygardsgaten 112, 5008 Bergen, Norway.
Email: role@norceresearch.no

Funding information
Research Council of Norway (NFR), Grant/Award Numbers: 297202/E10, 294742

Abstract

Total dissolved gas supersaturation from dams and power stations is a chronic freshwater pollutant that is toxic to animals with aquatic respiration. Laboratory ecotoxicology experiments have revealed capacity for captive fishes to saturoregulate by moving deeper, but field ecotoxicology research is largely lacking. We instrumented 94 brown trout in the Rysstad basin of the Otra River, Norway, with depth sensor acoustic transmitters and monitored their movements for 10 months. We found that the depths used by the trout largely protected them from the effects of total dissolved gas supersaturation, which ranged from 96% to 133% total gas pressure during the study. The depth use of fish was affected by sun position, lunar phase and spatial position in the river (i.e., available depth), and there was an extremely weak effect of total dissolved gas supersaturation that was counterintuitive (i.e., positive slope, movement toward surface). Depth traces of the fish revealed that nine fish died during the study, mostly coinciding with the first wave of supersaturation, consistent with observations of untagged dead fish with signs of gas bubble trauma found on the river bottom during this period (May-June). Overall, tagged trout exposure to total dissolved gas supersaturation depended on their use of depth, but responses to waves of extreme supersaturation at supraphysiological levels were weak and biologically insignificant, with individual variation and spatial position in the river most important in the model. Exposure to total dissolved gas supersaturation was mediated by individual differences in habitat use, which may be linked to activity and other traits that determine overall vulnerability to exposure to total dissolved gas supersaturation.

KEYWORDS
acoustic telemetry, generalized additive model, hydropower, pollution, river regulation

1 | INTRODUCTION

Point source pollutants in rivers negatively affect species' habitat quality and their physiology (Dudgeon et al., 2006; Jeffrey et al., 2015; Reid et al., 2019). However, water supersaturated with total dissolved gas is a poorly documented freshwater toxicant, which occurs most frequently in nature as a byproduct of hydroelectric generation (Pleizier, Algera, et al., 2020; Weitkamp & Katz, 1980). Water at atmospheric pressure is normoxic, but if mixed with air under added pressure, water can dissolve additional gas and become supersaturated relative to atmospheric pressure. This supersaturation commonly occurs below spillways of high dams or when flowing water is passed through tunnels and turbines, where it is pressurized and may dissolve additional gas if entrained. As supersaturated water flows downstream, it degasses at a rate that depends on a variety of environmental factors, especially mixing of the water column, and contact area at the air–water interface (Colt, 1986). Supersaturated water is toxic to many aquatic animals, causing the integration of gas bubbles in blood and tissues resulting in gas bubble disease (Pleizier, Algera, et al., 2020; Stenberg et al., 2020; Weitkamp & Katz, 1980).

Fish that are chronically exposed to supraphysiological (i.e., above physiological tolerance) levels of total dissolved gas supersaturation will eventually die, and high levels (i.e., >110% total gas pressure [TGP] in Atlantic salmon) in rivers can cause mortality of the wild animals that contract gas bubble disease (Pleizier, Algera, et al., 2020; Stenberg et al., 2020). Total dissolved gas supersaturation is most extreme at the water surface and attenuates at depth due to hydrostatic pressure (Pleizier, Nelson, et al., 2020). Fish may therefore find refuge by moving deeper or downstream to areas that are less affected. We therefore define saturoregulation as the active response by animals to limit exposure to total dissolved gas supersaturation. Laboratory ecotoxicology has suggested behavioural saturoregulation of some fish species that move deeper when exposed to supersaturated water (Wang et al., 2015). For rainbow trout (*Oncorhynchus mykiss*), coho salmon (*Oncorhynchus kisutch*), sockeye salmon (*Oncorhynchus nerka*), Chinook salmon (*Oncorhynchus tshawytscha*) and rock carp (*Procypris rabaudi*), active avoidance behaviour has been suggested with species-specific responses (Dawley et al., 1976; Stevens et al., 1980; Wang et al., 2015). However, there are relatively few field studies on the behaviour of wild fish encountering supersaturation in their natural habitat. What has been observed is that salmonids are often swimming deep enough to compensate for low levels of supersaturation (Johnson et al., 2007; Weitkamp et al., 2003). In field trials, Chinook salmon and rainbow trout in a river travelled deep enough to avoid acute gas bubble disease (Beeman & Maule, 2006). For brown trout (*Salmo trutta*) and Atlantic salmon (*Salmo salar*), avoidance behaviour to supersaturation has not been researched at all.

High-resolution monitoring of fish behaviour is possible with acoustic telemetry, which can be used to investigate relationships between individual animals and their environment (Hellström et al., 2016; Taylor et al., 2018), particularly how they respond to putative environmental stressors (e.g., Filous et al., 2017; Zięba et al., 2014). Brown trout in the Rysstad basin of the Otra River live in a 21-km stretch of river that is highly impacted by total dissolved gas supersaturation caused by the Brokke powerstation (Pulg, Stranzl, et al., 2016; Stenberg et al., 2020). We predicted that individual trout depth distributions would respond to ambient total dissolved gas supersaturation and considered putative predictors of depth distribution (solar azimuth, lunar phase and day of year) with total dissolved gas supersaturation to test this prediction. To generate data on the field ecotoxicology of total dissolved gas supersaturation, we instrumented 94 brown trout with acoustic depth transmitters in an array of acoustic receivers. We monitored the animals for 10 months as light, temperature and total dissolved gas supersaturation fluctuated, and we modelled individual movements to determine how the fish responded to the change to gas saturation in the river.

Significance

Hydropower is pervasive in rivers around the world and can cause total dissolved gas supersaturation, which is toxic to organisms using aquatic respiration. This research provides the most comprehensive assessment of the effects of total dissolved gas supersaturation on activity and behaviour of a riverine fish. Using acoustic telemetry, we show how brown trout have the potential to be vulnerable throughout the year to this toxic effluent but generally live at depths that compensate for the most toxic effects. The research is relevant for industry operations and government oversight of power production in rivers and provides a framework for using telemetry to study total dissolved gas supersaturation's impact on animals in rivers.

2 | METHODS

2.1 | Study site

The Otra River is an ultraoligotrophic river in southern Norway. Upper reaches of the river in the study area at the Rysstad (pronunciation: roo-stah) impoundment below Brokke power plant are home primarily to resident brown trout (*S. trutta*). The river is highly developed for hydropower and has a series of dams and weirs that regulate the water discharge, resulting in a variety of environmental changes that has altered the biology of the river (Wright et al., 2017).

This study was conducted in the Rysstad Basin, an impoundment between the outlet of the Brokke power station and the Tjurrmo dam in the Otra River (Figure 1). The aquatic macrophyte *Juncus bulbosus* (L.) has flourished in the upper reaches where depth is regulated and sediments are collected on the bottom (Velle et al., 2021). The hydropower generating station at Brokke is a source of aquatic total dissolved gas supersaturation (Pulg, Stranzl, et al., 2016; Pulg, Vollset, et al., 2016). River flow is strongly regulated and follows the production scheme at Brokke hydroplant 2 km upstream (330 MW, max. turbine discharge 136 m^3 s^{-1}). Gas saturation levels in the study period in the river were measured as high as 205% TGP at the power outlet with the largest peaks from April to June and again in December (earlier studies measured up to 176%; see Pulg, Stranzl, et al., 2016; Pulg, Vollset, et al., 2016). Supersaturation peaks reached up to 150% TGP when entering the 9-km-long impoundment and up to 130% at the end (Pulg et al., 2018; Pulg, Stranzl, et al., 2016; Pulg, Vollset, et al., 2016).

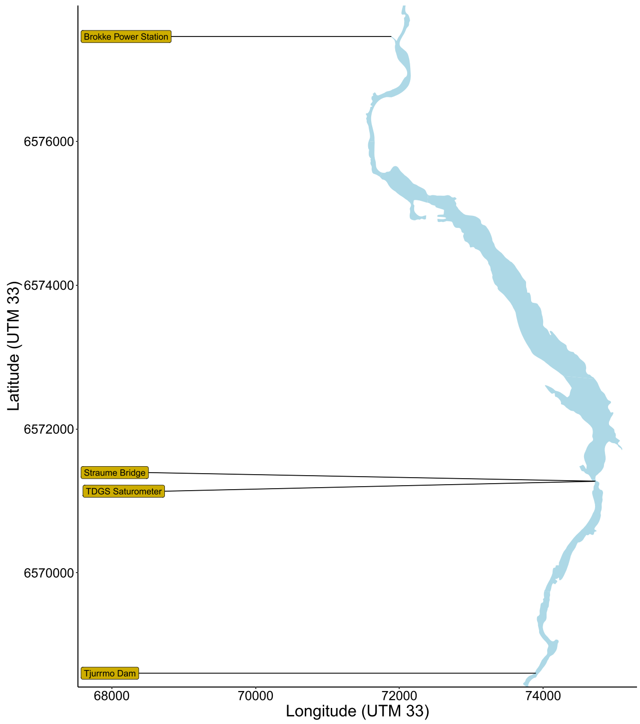

FIGURE 1 Map of the Rysstad basin in the Otra River and the telemetry array design. Receivers were arranged in two areas, with 20 in the upstream reach and 24 in the downstream area. One receiver was placed at a northern boundary to capture dispersal upriver. The navigable section of the river is truncated by the Tjurrmo dam at the lower end of the figure. Gas was logged at the Straume bridge, noted in yellow

2.2 | Study design

Ninety-four brown trout (238 ± 23 SD mm TL) were captured within the study reach in March–May 2020 by fyke net and beach seine net. All trout were held in keep nets for up to 48 h following capture prior to tagging. Depth sensor transmitters (Model D-2MP7, 32-mm length, 7-mm diameter, 3.7 g in air, 60- to 120-s transmission interval, 69-kHz frequency, 0- to 25.5-m depth range [0.1-m resolution], 10.6-month tag life; Thelma Biotel, Trondheim, Norway) were surgically implanted in the body cavity of brown trout. Veilleux et al. (2016) suggested that manufacturer calibrations are sufficient for similar depth sensors and no additional calibrations were performed. We calculated depth from pressure assuming 100 kPa at the water surface. Water level fluctuations were not accounted for given that the depth sensors would account for these changes. Trout were anaesthetized with benzocaine (0.25 ml L^{-1}) and transferred to a surgery table where an experienced surgeon opened the body cavity, inserted the sterile tag and sutured the incision site with two single interrupted sutures (4–0 Ethicon Vicryl synthetic absorbable suture and surgery time was <5 min). Fish were recovered in an aerated container for a minimum of 6–8 h and released under cover of darkness (∼2100 h). Batches were released at six different locations, all within receiver detection range.

Two acoustic receiver (Thelma TBR700, Thelma Biotel, Trondheim, Norway) arrays were established in the Rysstad basin to listen for tagged trout. Receivers were mounted on concrete anchors and placed on the river bottom. An array of receivers was established below the Straume bridge (Figure 1) in a lattice configuration. The downstream end of the array was at the Tjurrmo dam, which restricts live fish passage in both directions. An additional array of receivers was established upstream of the Straume bridge in a shallow area characterized by abundant *J. bulbosus*. Receivers were active from 16 March 2020 to 16 February 2021.

2.3 | Total dissolved gas supersaturation monitoring

Total dissolved gas supersaturation was measured with saturometers from Fisch- und Wassertechnik with an accuracy of ±SD 1% TGP and a measuring range from 80% to 250% TGP. The measuring principle is based on gas diffusion through a semipermeable membrane (adapted Weiss saturometer; Pulg, Stranzl, et al., 2016; Pulg, Vollset, et al., 2016). Logging interval was 30 min. The gas monitoring was conducted from 4 March 2020 to 12 February 2021 at the Straume bridge station, which was closest to the telemetry sites. An additional logger was placed in an upstream reach but did not measure any reliable values. The probes were pre-calibrated by the manufacturer and recalibrated at atmospheric pressure before deployment and when maintaining them (3-month intervals). They were mounted in 0.5-m depth at lowest water level and were up to 1.5 m deep when the impoundment was at maximum fill. The probes could not be mounted deep enough to avoid bubble formation by compensation depth due to limited water depth. Instead, they were mounted directly in the main current and were exposed to the water stream. Thus, bubble formation on the probe and a potential bias were avoided as confirmed by visual checks and control measurements with a handheld logger when installing and maintaining the logger. One saturometer logger was placed directly at the hydroplant outlet 'Brokke', one was deployed at the Straume bridge (8 km below Brokke in the middle of the impoundment) and one was placed 11 km below Brokke at the Tjurrmo dam, the lower end of the impoundment (Figure 1).

The temperature data ranged from 0°C to 14.2°C from 4 March 2020 to 12 February 2021. The average in this period was 5°C.

2.4 | Data preparation

Data were offloaded from all receivers in February 2021. Solar and lunar data were extracted for Rysstad and synchronized with the detection times using the suncalc (Thieurmel & Elmarhraoui, 2019) and lunar (Lazaridis, 2014) packages in R (R Core Team, 2020). The S256 protocol is prone to false detections, and we therefore calculated cost distances between receivers using the costDistance function in the raster package (Hijmans, 2020) and the gLength function in gdistance (van Etten, 2017). Cost distances > 3 km were removed given that it would be unlikely for an individual to move that distance without being detected by another receiver. Detections for which there were fewer than two detections for an individual on a receiver in a 5-min interval were also removed. Each detection was matched to the ambient gas saturation value at the Straume bridge station within the 30-min window of recording. Visual inspection of individual depth profiles revealed nine individuals that likely died or discarded the tag during the study and within the receiver range, with constant flat lines of depth suggesting that the tags were settled on the river bottom. Date of death was determined visually, and the depth traces were clipped to exclude depth recordings that were inferred to represent immotile tags. Data were plotted using ggplot2 (Wickham, 2016).

2.5 | Data analysis

2.5.1 | Depth response to total dissolved gas supersaturation

Data were modelled with hierarchical generalized additive models (GAM; Pedersen et al., 2019) using the *bam* function in the mgcv package (Wood, 2017). We hypothesized that trout depth selection would be affected by ambient total dissolved gas supersaturation, sun position, lunar illumination and date. Because the sun position (we selected solar azimuth) is cyclical, we modelled it with a cyclic cubic regression spline (*bs* = *'cc'*). Day of the year was also a smooth function but not cyclic cubic because we did not have observations through the full year. Lunar illumination and total dissolved gas supersaturation were linear variables. Individual was considered as a random intercept. We also incorporated a temporal autocorrelation structure. In *bam*, the temporal autocorrelation can be modelled by a parameter *rho*, which we calculated from a model without autocorrelation and then input in the subsequent model as the *rho* parameter with start times specified for the first observation made of each individual. The model with and without the *rho* parameter was compared by Akaike information criterion (AIC; Baayen et al., 2018). We also predicted that there would be a spatial component to the individual's depth use because of different depths available in the river and incorporated a bivariate spatial smoother of longitude and latitude in the model to account for the fact that the fish's depth would depend on its spatial position in the river driving different depths available. The final model was therefore *bam(depth ∼ ambient_gas) + s(longitude, latitude) + s(solar_azimuth, bs = 'cc') + s(day) + lunar_illumination + s(ID, bs = 're'), rho = rho_estimated*.

2.5.2 | Risk model

Pleizier, Nelson, et al. (2020) presented an equation for rainbow trout (*O. mykiss*) suggesting that each metre depth reduces exposure to total dissolved gas supersaturation by 9.7%. We estimated exposure to total dissolved gas supersaturation of each individual based on the ambient gas levels and individual depth resolved by the acoustic receivers. So that each detection was assigned a binary risk, either the fish was in a two-dimensional position (depth and time) exposed to total dissolved gas supersaturation > 100% or not. Although most clinical signs of gas bubble disease are observed following exposure to higher levels of total dissolved gas supersaturation, we wanted to model any exposure levels in consideration of sublethal effects and carryover effects that can occur from prolonged exposure and poor avoidance. The logistic risk was modelled as a hierarchical generalized additive model with a binary response. The model asked whether ambient total dissolved gas supersaturation, spatial coordinates *s(longitude, latitude)*, sun position *s(solar_azimuth, bs = 'cc')*, day of year *s(day)* or individual *s(ID, bs = 're')* affected the probability of risk of supersaturation exposure. The model structure was therefore essentially equivalent to the depth model described above, but we excluded the linear term for lunar illumination. In consideration of temporal autocorrelation, a null model was once again run to estimate a *rho* parameter, which was included in a subsequent model and compared to the null by AIC.

3 | RESULTS

Average total dissolved gas supersaturation in the river at the logging station was 106 ± 8% (Figure 2). Total dissolved gas supersaturation in Rysstad was below 110% TGP through mid-April. On 27 May, the first peak recorded >130% total dissolved gas supersaturation, followed by peaks > 130 total dissolved gas supersaturation on 15, 16 and 18 June (Figure 3). Despite releasing all 94 trout directly into the receiver array, only 93 fish were reliably detected during the study. Durations of detection were on average 95 ± 80 SD days, with nine fish detected for <10 days. Given there was suitable habitat uncovered in the area, it is likely that some fish dispersed from the release site into different areas, especially given that most individuals were not captured directly in the areas where they were released after tagging. Nevertheless, about a third of the fish were detected for intervals > 100 days, yielding 1.57 million detections after filtering for likely false and unreliable detections. Average depth use in the study was 3.53 ± 2.43 SD m deep. One of the trout was recaptured by a local artisanal fisher in a fyke net and removed from the study on 16 October in a batch of 241 trout; likely, others were caught and not noticed given that high volumes in which fish were captured in July–October. Nine trout were determined to have died during the study based on depth traces within the array, on 23, 24 and 30 May (two individuals), 3, 6 and 25 June, 7 July and 10 August (Figure 3). These deaths occurred several months after tagging and mostly during a period of high ambient total dissolved gas supersaturation. It was not obvious that the fish that died lived more shallow than those that did not (Figure 5), nor whether they spent more time in the upper reach with higher TGP levels (higher latitude; see Figure 4). There was an overall decline in the number of individuals detected per day after June when the supersaturation stabilized following a month of extremes (Figure 3). There were likely other individuals that died

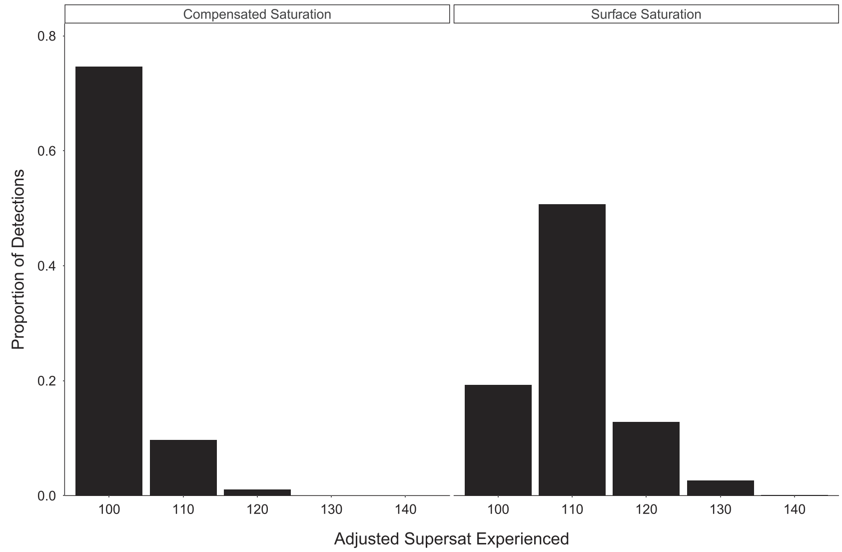

FIGURE 2 Proportion of detections in Rysstad basin (Otra River) during the study given the surface supersaturation measured at the Straume bridge and recalculated based on the depth of the detection. Saturation levels are ceiling rounded

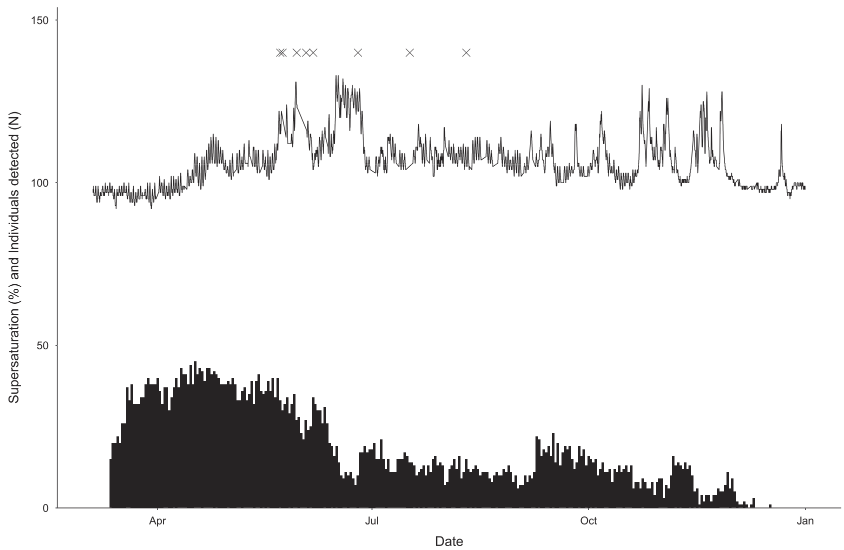

FIGURE 3 Number of individual fish detected in the Rysstad system on acoustic receivers by day of the year during the study (bars). Overlaid (line) is the total gas pressure supersaturation (%) of the water measured at the gas logging station at the Straume bridge (Figure 1). Nine individuals were confirmed to have died; the timing of death is noted by ex symbols on the top of the figure (×)

outside the array, but these could not be separated from individuals that dispersed from the array, so no effort was made to estimate their fate.

3.1 | Depth response to total dissolved gas supersaturation

The model with and without the *rho* parameter had essentially identical results, but the model with the *rho* parameter was better according to AIC (ΔAIC = 48,139). The model intercept was at −3.68, suggesting that the baseline expected depth of fish was >3 m. Individual random intercepts suggested depth adjustments to account for individual variation ranging from +2.67 to −8.95 m, emphasizing individual differences from the intercept. The depth of the trout in Rysstad responded to multiple environmental cues. Most strongly, depth was a function of the solar azimuth; fish were deepest at midday and came shallower in the evening and at night. The depth adjustment was up to 0.87 m deeper between the midday sun and crepuscular values ($F = 849{,}147$, $P < 0.01$; mean standard error of smoother values = 0.0077). The day-of-year smoother was also significant, showing a declining depth through the year ($F = 1875$, $P < 0.01$; mean standard error of smoother values = 0.0135). The linear effect of lunar illumination was significant ($t = 19.52$, $P < 0.01$) with a positive slope ($b = 0.08 \pm 0.004$ SE). The linear effect of total dissolved gas supersaturation was also significant ($t = 2.46$, $P = 0.01$) but with a very weak overall effect suggestive of about a 0.8 ± 0.3-SE-cm shallower depth for each 10% increase in total dissolved gas supersaturation, the opposite direction to what was expected but biologically minuscule in terms of magnitude.

3.2 | Risk model

The binomial risk model fit better when the *rho* parameter was integrated to account for temporal autocorrelation (ΔAIC = 1,111,743).

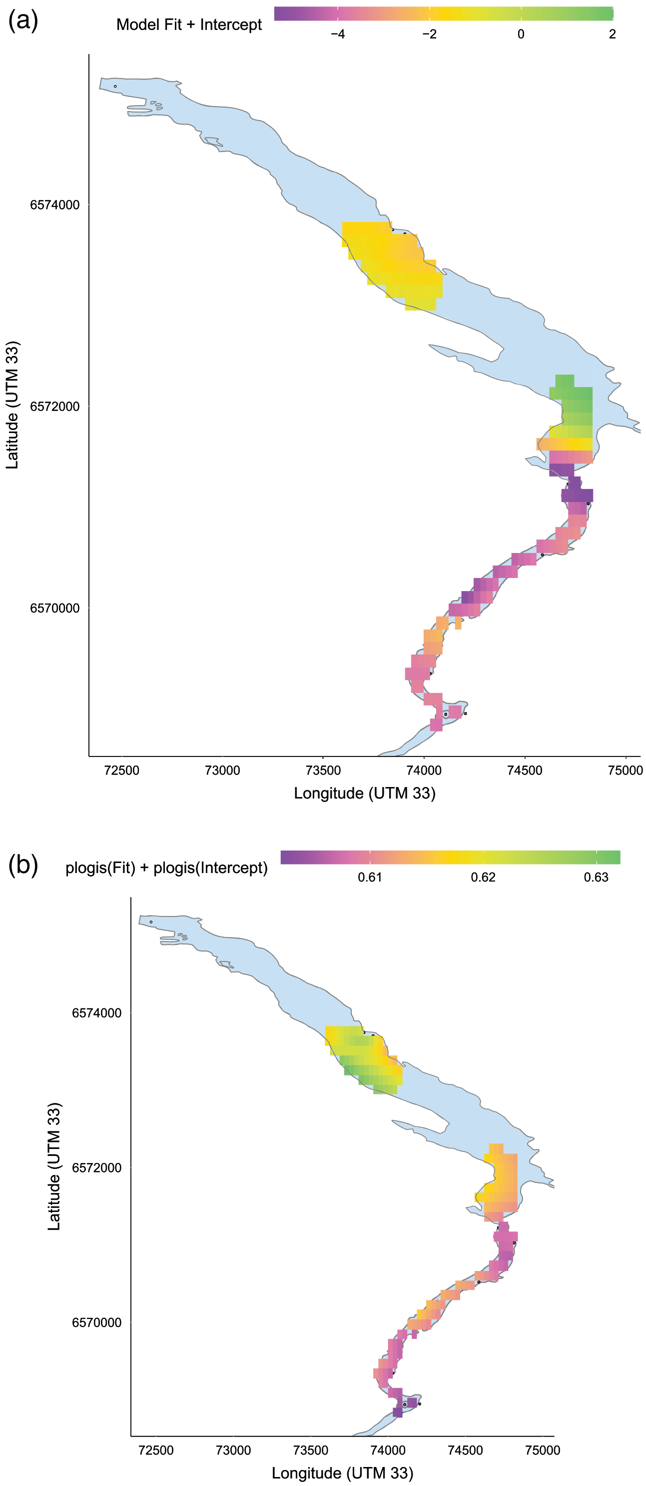

FIGURE 4 Posterior predictions of spatial effects on depth (a) and risk of supersaturation exposure (b) in Rysstad. Depth values are presented in metres and are adjusted based on the model intercept, and risk values are logistic transformed. The northern array is an area where depths are known to be shallow and where risk of exposure to total gas pressure > 100% is higher. Risk values are presented as probability of exposure to TDG > 100%, with higher values corresponding to the shallower areas

Individual random effects in the model were important, suggesting that individual fish had adjusted logistic transformed probabilities ranging from 0.47 to 0.64 of risk to exposure to gas >100%. The risk model revealed a significant spatial effect (Figure 4), which suggested higher risk in the upper reaches (maximum logistic transformed fitted value = 0.63) that are shallower and therefore more exposed to supersaturation than the lower latitudes (minimum logistic transformed fitted value = 0.60). Interestingly, random effects suggested that the nine individuals that most likely died were not among the highest individuals at risk (Figure 5). Fitted values transformed by the logistic function suggested a change in risk of approximately 10% in the northern array compared to the area covered by the southern array (Figure 4). Sun position also exerted a significant effect on risk of supersaturation ($F = 29{,}557$, $P < 0.01$), suggesting that trout were more exposed to supersaturated water when the sun was low (i.e., night-time), which corresponds to their diel vertical movements in the water column (see 'depth response'). However, the changes were biologically meaningless, with changes in risk of exposure shifting between 0.53 and 0.56 with different solar positions. The linear effect of gas, however, had a significant influence ($t = 521$, $P < 0.01$); exponentiating the coefficient yielded an odds ratio of 1.02, suggesting that each unit increase in total dissolved gas supersaturation increased odds of exposure by 2%. Risk of exposure to total dissolved gas supersaturation was higher as total dissolved gas supersaturation increased.

4 | DISCUSSION

4.1 | Main effects

Hierarchical generalized additive modelling revealed a clear pattern in depth use of trout that followed solar and lunar cues but was weakly affected by total dissolved gas supersaturation, contrary to our prediction. There was a weak but significant effect of ambient total dissolved gas supersaturation on depth use of trout such that trout tended to be shallower at higher values of total dissolved gas supersaturation, but the slope of 0.001 indicated negligible changes and the intercept at 3.76 m suggested that changes would not have meaningfully affected exposure due to deep compensation depth. Total dissolved gas supersaturation fluctuated throughout the study, reaching concentrations up to 133% at the Straume gas logging station.

Some laboratory experiments suggest that fish will move deeper when exposed to total dissolved gas supersaturation (Wang et al., 2015), but the experimental design seems to be important as well as species and level of TDGS. Lund and Heggberget (1985) observed no depth compensation among rainbow trout held in tanks but high mortality if the tanks were shallow (max depth = 0.4 m). Similarly, the location where trout live in the river will affect their total dissolved gas supersaturation experience. Spatial smoothers in the model showed that the depth used in upper reaches was shallower, undoubtedly because the maximum available depth is shallower in this area (max depth = 3 m). Fish in upper reaches must therefore be more

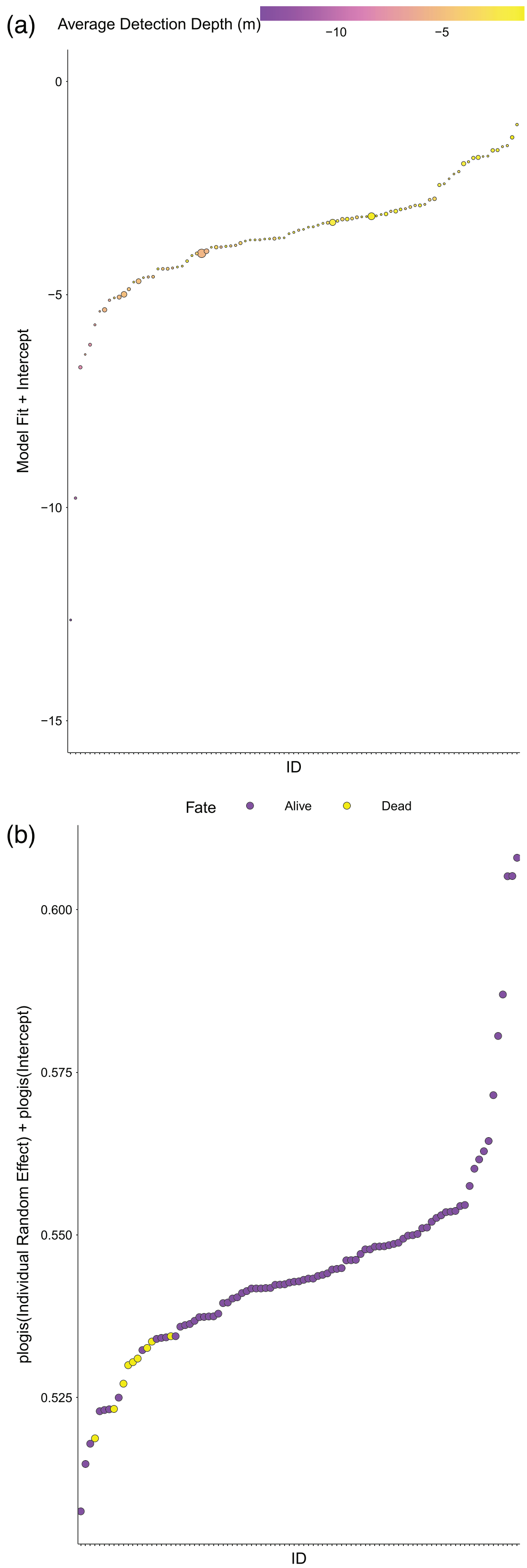

FIGURE 5 Both model random effects distributions. Values indicate individual random effects adjusted to account for model intercept, indicating individual variation. Individual points are coloured for the main depth model (a) based on the individual's mean depth during the study and scaled to size based on the number of detections for that ID. For the risk model (b), points are coloured based on whether the individual was one of the nine fish determined to have died during the study (yellow). Note that most of the fish that died were not considered themselves to be high based on their depth and the ambient supersaturation at each detection. In both figures, each point represents one unique individual in the study

vulnerable to the effects of total dissolved gas supersaturation, which is exactly what we observed in the risk model where *plogis* transformed values indicated about a 10% increase in risk of exposure for fish in upper reaches. However, all the trout were highly mobile in the system and many moved between these reaches with regularity. We expected fish in these upstream reaches would move downstream at high total dissolved gas supersaturation waves, similar to the horizontal avoidance responses of cyprinids reported by Wang et al. (2015), or to greater depth as suggested by Dawley et al. (1976); however, this was generally not the case. Avoidance responses were overall weak at best when supersaturation was high in Rysstad.

Few field studies of wild fish have been conducted to examine the behaviour of free living fish in areas afflicted with total dissolved gas supersaturation, and none with high resolution monitoring of fish depth use as made possible by our extensive acoustic tracking array. Weitkamp et al. (2003) tracked behaviour of seven fish species using radio transmitting depth sensors and calculated mean depth use on 11–135 relocations (mean relocations per species), finding that most of the time fish were about 2 m or deeper from the surface, protected from total dissolved gas supersaturation < 120% TGP at the surface. In our study, trout were similarly distributed away from the surface and most of the time were entirely unexposed to total dissolved gas supersaturation due to compensation depth, even if it was occurring at the surface. Trout were especially deep during daylight hours, probably close to the bottom and in refuge, and were therefore less exposed to supersaturation at these hours. Hydropower regimes and saturopeaking (i.e., acute pulses of supersaturated water; Pulg, Stranzl, et al., 2016; Pulg, Vollset, et al., 2016) may therefore have implications for exposure of trout to supersaturation and gas bubble disease risk if saturation is peaking at night when trout are higher in the water column. Indeed, our risk model suggested a high risk of exposure to total dissolved gas supersaturation for fish when the sun was low, corresponding to their diel shifts in depth use. The changes in risk in our study were too small to conclude that they were meaningful; however, the risk may potentially be meaningful in more shallow reaches and at higher TGP. Evidence from the data (i.e., vertical and horizontal movement) suggested that the trout did not modulate their behaviour during total dissolved gas supersaturation waves, still exhibiting a shift towards the surface at night that increased risk of exposure to gas saturation > 100%. Trout occurred deep enough to compensate for total dissolved gas supersaturation most of the time, but very likely due to other reasons than gas avoidance behaviour based on general trout behaviour and relationships between depth and other variables in our analysis. Evidence of active saturoregulation was not found.

Overall, the results revealed generally low exposure to total dissolved gas supersaturation in Rysstad, which was surprising given the high levels of supersaturation downstream of the power plant. The depth model intercept suggested that trout were generally found below 3 m, which was then affected by the sun position, time of year, individual random intercepts, and spatial position in the river according to the bivariate smoother. Depths > 3 m would have compensated for all levels of total dissolved gas supersaturation, although such depths were not always available where receivers were placed. The risk model emphasized that spatial positions (i.e., deep or shallow areas) and individual random effects were key drivers of exposure to supersaturation among individuals. During the peak of the total dissolved gas supersaturation wave in June, visual observations confirmed mortality of (presumably) untagged trout on the bottom of the river and local catches of trout in fyke nets indicated symptoms of gas bubble disease. Fish mortality was observed in the upper part of the basin, which is shallower and therefore depth compensation potential is limited. Despite these findings, there is no doubt that the trout population in Rysstad is affected by gas bubble disease and the effects of total dissolved gas supersaturation from the power station upstream.

Several fish that died during May and June could have succumbed to gas bubble disease; indeed, two fish died on 30 May following the first peak > 130% in total dissolved gas supersaturation on 29 May, we cannot rule out that this was a coincidence, but it aligns with our a priori hypothesis that total dissolved gas supersaturation would have acute lethal consequences to the tagged fish. We predicted that there would be clear patterns of avoidance among the trout in the study revealed by changes in the vertical profile of trout when supersaturation arrived or downstream dispersal. Trout were mobile within the system and could easily move upstream or downstream from shallow to deep areas where supersaturation is negated by depth. However, even during high peaks, trout were present in the upstream reaches of the river where depths < 2 m would not have provided suitable refuge to supersaturation > 130% at the surface based on 9.7% compensation per metre depth (Pleizier, Nelson, et al., 2020).

Solar azimuth had a profound influence on depth use by the trout, suggesting some diel variation in individual patterns of habitat selection consistent with what has been observed for anadromous trout (Eldøy et al., 2017; Kristensen et al., 2018). The *bam* model suggested that trout were deeper when the sun was highest by about 50 cm, in the middle of the day, and shallower during night-time by about 35 cm, relative to the intercept. There is a broad literature on activity levels of brown trout and inconsistencies regarding when they feed, and on what (reviewed by Klemetsen et al., 2003). Generally, they are viewed as sit-and-wait predators in streams that feed on drifting macroinvertebrates with higher activity levels nocturnally and at the crepuscule (Giroux et al., 2000). Insects may preferentially drift nocturnally to avoid trout predation (Flecker, 1992), but this does not necessarily explain why trout were consistently shallower at night than during the day. Similar patterns of diel vertical movements are usually attributed to predation risk, which may also be a driver of depth use in Rysstad. Intuitively, the two-dimensional spatial smoothers in the model suggested that depth use was shallower in the upper river reaches where the maximum depths were $\sim$2.5 m, compared to the lower reaches of the river where depths were up to 12 m.

Modelling animal movement using acoustic telemetry detections is challenging and requires careful consideration of model parameterization. We modelled depths throughout the study period for multiple fish, which seriously violate assumptions of independence. Depth in the system has spatial dependency because of different areas having different depth available to individuals, which is why we included the bivariate spatial smoother in the model. Depth of an individual is also serially autocorrelated because the depth of the fish is more similar to the most recently recorded depth. Including the *rho* parameter in the model to account for residual autocorrelation improved the model considerably but had no effect on the model interpretation. We explored other options including using the *gamm* framework, which uses nlme and the more common corAR1 and corARMA residual autocorrelation structures, but our data were too large to fit with that model. We also considered using R-INLA and generating a mesh of receivers to estimate residual autocorrelation, but this also would not fit. The *bam* model predicted spatial effects on the intercept between $+3$ (in the upper reaches) and -2 (at the deepest point in the array), suggesting that it appropriately attributed variation in depth of fish to the spatial dimensions, appropriately partitioning variance and helping make more robust conclusions about the effects of total dissolved gas supersaturation on fish depth.

4.2 | Further research

The majority of research on total dissolved gas supersaturation and its effects on fish has focused on laboratory experiments testing the time to mortality for different life stages of different species at different gas saturations (examples reviewed by Pleizier, Algera, et al., 2020). The present study is among the first (see Weitkamp et al., 2003) and most detailed field studies but does not answer all possible questions. We were not able to establish a control site to compare the depth distribution of trout in unaffected areas, which would have increased power to draw conclusions about the response of individuals to the polluting gas.

Phenotyping and genotyping individuals prior to tagging (i.e., behavioural syndrome and metabolism) could explain more about the behaviour and survival of fish encountering total dissolved gas supersaturation. Random intercepts for each individual indicated that there was important inter-individual variation in depth use and the risk model corroborated this with random intercepts also indicating that some fish were more prone to exposure to total dissolved gas supersaturation than others. There may also be some evolutionary pressures on fish living in rivers such as Rysstad where total dissolved gas supersaturation has been present for several decades that selects for genes or phenotypes that are resilient to supersaturation; Gray et al. (1982) suggested that higher supersaturation tolerance among Columbia River fish compared to controls from Italy might reflect a legacy of exposure in the Columbia. Cyprinids have better physiological tolerance to total dissolved gas supersaturation than salmonids (e.g., Fan et al., 2020; Wang et al., 2015), but what the mechanisms and whether they are heritable could be revealed in experiments and could include some experimental displacement field studies by transporting, tagging and observing behaviour and survival of fish from an affected and unaffected area. Matching our findings to observations of high mortality and symptoms of gas bubble disease of fish in the Otra River, however, are not in support of a hypothesis that this population is especially resilient to the trauma caused by total dissolved gas supersaturation.

4.3 | Applications

Not all power stations are equally prone to supersaturating water; certain hydroelectric turbines, dam head heights and intakes may enhance risk of supersaturation. Supersaturation in Rysstad tends to peak in spring, when fish are beginning to disperse as water warms, and autumn around when fish are moving and preparing to spawn. There were some seasonal trends suggesting shallower depth use of trout during these transitional seasons compared to summer, when trout depths tended to be slightly deeper according to the generalized additive model (GAM) model.

Trout that move vertically in the water column must be slightly more vulnerable to supersaturation at night than during the day, but the risk model suggested that diel differences in risk of exposure were negligible. Ultimately, individual differences seem to result in more extreme differences in depth use and risk of supersaturation exposure than the diel periodicity. During our study, at least nine of the 94 tagged trout died, and there was an abrupt reduction in the number of fish detected after July when the spring supersaturation wave receded, suggesting that supersaturation could be attributed to mortality of >10% of our study animals.

Management tends to focus on the population scale, which is robust for the trout in Rysstad; however, individual welfare is also considered part of the purview of managers (Papastavrou et al., 2017). Gas bubble disease is a traumatic affliction that causes fish to suffer injuries and death (Pleizier, Algera, et al., 2020; Pleizier, Nelson, et al., 2020). Ultimately, we found no evidence that the trout were saturoregulating in the system based on telemetry, suggesting that the fish mostly have suitable habitat refuge outside the highest areas of influence of supersaturation (<1 m) and that the actual supersaturation experienced by the animals during the study was predominantly ≤100% due to hydrostatic compensation. Despite these findings, observations of tagged and untagged fish dying and gas bubble disease in untagged fish captured by local fishers suggest that gas bubble disease is a welfare concern in the river and may represent additive mortality. Regulations should focus on limiting allowable gas effluent from power stations in Norway and be particularly diligent when rivers are shallow and have limited vertical refuge that fish will use to compensate for the toxic effects of total dissolved gas supersaturation.

ACKNOWLEDGEMENTS

We gratefully acknowledge Reidar Tveit and his family for their assistance capturing fish, holding fish, and setting up our tagging station. We essentially would have been lost without his kindness and generosity. Benoit Demars assisted with fish capture and receiver maintenance and Susanne Schneider helped build receiver moorings. The power company Otra Kraft paid for some accommodation, tools for building receiver moorings, and boating. Otra Kraft did not have any influence or contribution to study design, data analysis, or interpretation of findings. The Research Council of Norway (NFR) projects SUPERSAT 294742: Hydropower induced supersaturation in freshwaters: effects on ecosystems, mitigation and solutions and MADMACS 297202/E10 supported the work. We gratefully acknowledge this stackexchange answer from Dr. Gavin Simpson that resolved some modelling questions during analysis (https://stats.stackexchange.com/questions/316396/built-a-covariance-matrix-for-gam-using-magic-and-magic-post-proc-now-how-to-ca).

DATA AVAILABILITY STATEMENT

Metadata and detection data will be publicly archived with the Ocean Tracking Network database (https://oceantrackingnetwork.org/). Metadata will additionally be available on Zenodo (https://zenodo.org/) where all the lead author's publication data are archived. Code will be made available on github for the lead author at https://github.com/robertlennox.

REFERENCES

Baayen, R. H., van Rij, J., de Cat, C., & Wood, S. (2018). Autocorrelated errors in experimental data in the language sciences: Some solutions offered by generalized additive mixed models. In *Mixed-effects regression models in linguistics* (pp. 49–69). Cham: Springer. https://doi.org/10.1007/978-3-319-69830-4_4

Beeman, J. W., & Maule, A. G. (2006). Migration depths of juvenile Chinook salmon and steelhead relative to total dissolved gas supersaturation in a Columbia River reservoir. *Transactions of the American Fisheries Society*, *135*(3), 584–594.

Colt, J. (1986). Gas supersaturation—impact on the design and operation of aquatic systems. *Aquacultural Engineering*, *5*(1), 49–85.

Dawley, E., Monk, B., Schiewe, M., Ossiander, F., & Ebel, W. (1976). *Salmonid bioassay of supersaturated dissolved air in water*. Ecological Research Series Report number EPA600/3-76-056. Duluth, Minnesota, USA: U. S. Environmental Protection Agency Office of Research and Development, Environmental Research Laboratory.

Dudgeon, D., Arthington, A. H., Gessner, M. O., Kawabata, Z. I., Knowler, D. J., Lévêque, C., Naiman, R. J., Prieur-Richard, A. H., Soto, D., Stiassny, M. L. J., & Sullivan, C. A. (2006). Freshwater biodiversity: Importance, threats, status and conservation challenges. *Biological Reviews*, *81*(2), 163–182. https://doi.org/10.1017/S1464793105006950

Eldøy, S. H., Davidsen, J. G., Thorstad, E. B., Whoriskey, F. G., Aarestrup, K., Naesje, T. F., Rønning, L., Sjursen, A. D., Rikardsen, A. H., & Arnekleiv, J. V. (2017). Marine depth use of sea trout *Salmo trutta* in fjord areas of central Norway. *Journal of Fish Biology*, *91*(5), 1268–1283. https://doi.org/10.1111/jfb.13463

Fan, Z., Deng, Y., Yuan, Q., Liu, X., Shi, H., Feng, C., Yang, Y., & Xu, L. (2020). Effect of total dissolved gas supersaturation on the tolerance of grass carp (Ctenopharyngodon idellus). *Environmental Sciences Europe*, *32*(1), 1–10.

Filous, A., Friedlander, A. M., Koike, H., Lammers, M., Wong, A., Stone, K., & Sparks, R. T. (2017). Displacement effects of heavy human use on coral reef predators within the Molokini Marine Life Conservation District. *Marine Pollution Bulletin*, *121*(1–2), 274–281. https://doi.org/10.1016/j.marpolbul.2017.06.032

Flecker, A. S. (1992). Fish predation and the evolution of invertebrate drift periodicity: Evidence from neotropical streams. *Ecology*, *73*(2), 438–448. https://doi.org/10.2307/1940751

Giroux, F., Ovidio, M., Phillippart, J. C., & Baras, E. (2000). Relationship between the drift of macroinvertebrates and the activity of brown trout in a small stream. *Journal of Fish Biology*, *56*(5), 1248–1257. https://doi.org/10.1111/j.1095-8649.2000.tb02137.x

Gray, R. H., Page, T. L., Saroglia, M. G., & Bronzi, P. (1982). Comparative tolerance to gas supersaturated water of carp, *Cyprinus carpio*, and black bullhead, *Ictalurus melas*, from the USA and Italy. *Journal of Fish Biology*, *20*(2), 223–227. https://doi.org/10.1111/j.1095-8649.1982.tb03922.x

Hellström, G., Klaminder, J., Jonsson, M., Fick, J., & Brodin, T. (2016). Upscaling behavioural studies to the field using acoustic telemetry. *Aquatic Toxicology*, *170*, 384–389. https://doi.org/10.1016/j.aquatox.2015.11.005

Hijmans, R. J. (2020). Raster: Geographic data analysis and modeling. R package version 3.4–5. https://cran.r-project.org/package=raster

Jeffrey, J. D., Hasler, C. T., Chapman, J. M., Cooke, S. J., & Suski, C. D. (2015). Linking landscape-scale disturbances to stress and condition of fish: Implications for restoration and conservation. *Integrative and Comparative Biology*, *55*(4), 618–630. https://doi.org/10.1093/icb/icv022

Johnson, E. L., Clabough, T. S., Peery, C. A., Bennett, D. H., Bjornn, T. C., Caudill, C. C., & Richmond, M. C. (2007). Estimating adult Chinook salmon exposure to dissolved gas supersaturation downstream of hydroelectric dams using telemetry and hydrodynamic models. *River Research and Applications*, *23*(9), 963–978. https://doi.org/10.1002/rra.1019

Klemetsen, A., Amundsen, P. A., Dempson, J. B., Jonsson, B., Jonsson, N., O'connell, M. F., & Mortensen, E. (2003). Atlantic salmon *Salmo salar* L., brown trout *Salmo trutta* L. and Arctic charr *Salvelinus alpinus* (L.): A review of aspects of their life histories. *Ecology of Freshwater Fish*, *12*(1), 1–59. https://doi.org/10.1034/j.1600-0633.2003.00010.x

Kristensen, M. L., Righton, D., del Villar-Guerra, D., Baktoft, H., & Aarestrup, K. (2018). Temperature and depth preferences of adult sea trout *Salmo trutta* during the marine migration phase. *Marine Ecology Progress Series*, *599*, 209–224. https://doi.org/10.3354/meps12618

Lazaridis, E. (2014). Lunar: Lunar phase & distance, seasons and other environmental factors (version 0.1–04). Available from http://statistics.lazaridis.eu

Lund, M., & Heggberget, T. G. (1985). Avoidance response of two-year-old rainbow trout, *Salmo gairdneri* Richardson, to air-supersaturated water: Hydrostatic compensation. *Journal of Fish Biology*, *26*(2), 193–200. https://doi.org/10.1111/j.1095-8649.1985.tb04256.x

Papastavrou, V., Leaper, R., & Lavigne, D. (2017). Why management decisions involving marine mammals should include animal welfare. *Marine Policy*, *79*, 19–24. https://doi.org/10.1016/j.marpol.2017.02.001

Pedersen, E. J., Miller, D. L., Simpson, G. L., & Ross, N. (2019). Hierarchical generalized additive models in ecology: An introduction with mgcv. *PeerJ*, *7*, e6876.

Pleizier, N. K., Algera, D., Cooke, S. J., & Brauner, C. J. (2020). A meta-analysis of gas bubble trauma in fish. *Fish and Fisheries*, *21*(6), 1175–1194. https://doi.org/10.1111/faf.12496

Pleizier, N. K., Nelson, C., Cooke, S. J., & Brauner, C. J. (2020). Understanding gas bubble trauma in an era of hydropower expansion: How do fish compensate at depth? *Canadian Journal of Fisheries and Aquatic Sciences*, *77*(3), 556–563. https://doi.org/10.1139/cjfas-2019-0243

Pulg, U., Stranzl, S., Vollset, K. W., Barlaup, B. T., Olsen, E., Skår, B., & Velle, G. (2016). *Gassmetning i Otra nedenfor Brokke kraftverk. Uni Research Miljø LFI rapport 271. Technical report*. Bergen: NORCE.

Pulg, U., Vollset, K. W., Velle, G., & Stranzl, S. (2016). First observations of saturopeaking: Characteristics and implications. *Science of the Total Environment*, *573*, 1615–1621. https://doi.org/10.1016/j.scitotenv.2016.09.143

Pulg, U., Vollset, W. K., Stranzl, S., Espedal, O. E., Hauer, C., & Floedl, P. (2018). *Gassovermetning i Otra nedenfor Brokke 2016–2017 og muligheter for avbøtende tiltak. Uni Research Miljø LFI rapport 319. Technical report*. Bergen: NORCE.

R Core Team. (2020). *R: A language and environment for statistical computing*. Vienna, Austria: R Foundation for Statistical Computing. https://www.r-project.org/

Reid, A. J., Carlson, A. K., Creed, I. F., Eliason, E. J., Gell, P. A., Johnson, P. T., Kidd, K. A., MacCormack, T., Olden, J. D., Ormerod, S. J., Smol, J. P., Taylor, W. W., Tockner, K., Vermaire, J. C., Dudgeon, D., & Cooke, S. J. (2019). Emerging threats and persistent conservation challenges for freshwater biodiversity. *Biological Reviews*, *94*(3), 849–873. https://doi.org/10.1111/brv.12480

Stenberg, S. K., Velle, G., Pulg, U., & Skoglund, H. (2020). Acute effects of gas supersaturation on Atlantic salmon smolt in two Norwegian rivers. *Hydrobiologia*, 1–12. https://doi.org/10.1007/s10750-020-04439-z

Stevens, D. G., Nebeker, A. V., & Baker, R. J. (1980). Avoidance responses of salmon and trout to air-supersaturated water. *Transactions of the American Fisheries Society*, *109*(6), 751–754.

Taylor, M. D., van der Meulen, D. E., Brodie, S., Cadiou, G., & Knott, N. A. (2018). Applying acoustic telemetry to understand contaminant exposure and bioaccumulation patterns in mobile fishes. *Science of the Total Environment*, *625*, 344–354. https://doi.org/10.1016/j.scitotenv.2017.12.177

Thieurmel, B., & Elmarhraoui, A. (2019). Suncalc: Compute sun position, sunlight phases, moon position and lunar phase. R package version 0.5.0. https://cran.r-project.org/package=suncalc

van Etten, J. (2017). R package gdistance: Distances and routes on geographical grids. *Journal of Statistical Software*, *76*(1), 1–21. https://doi.org/10.18637/jss.v076.i13

Veilleux, M. A., Lapointe, N. W., Webber, D. M., Binder, T. R., Blanchfield, P. J., Cruz-Font, L., Wells, M. G., Larsen, M. H., Doka, S. E., & Cooke, S. J. (2016). Pressure sensor calibrations of acoustic telemetry transmitters. *Animal Biotelemetry*, *4*(1), 1–8. https://doi.org/10.1186/s40317-015-0093-0

Velle, G., Skoglund, H., & Barlaup, B. T. (2021). Effects of nuisance submerged vegetation on the fauna in Norwegian rivers. *Hydrobiologia*. https://doi.org/10.1007/s10750-020-04465-x

Wang, Y., Li, K., Li, J., Li, R., & Deng, Y. (2015). Tolerance and avoidance characteristics of Prenant's schizothoracin *Schizothorax prenanti* to total dissolved gas supersaturated water. *North American Journal of Fisheries Management*, *35*(4), 827–834. https://doi.org/10.1080/02755947.2015.1052160

Weitkamp, D. E., & Katz, M. (1980). A review of dissolved gas supersaturation literature. *Transactions of the American Fisheries Society*, *109*(6), 659–702. https://doi.org/10.1577/1548-8659(1980)109<659:AROGDS>2.0.CO;2

Weitkamp, D. E., Sullivan, R. D., Swant, T., & DosSantos, J. (2003). Behavior of resident fish relative to total dissolved gas supersaturation in the lower Clark Fork River. *Transactions of the American Fisheries Society*, *132*(5), 856–864. https://doi.org/10.1577/T02-025

Wickham, H. (2016). *ggplot2: Elegant graphics for data analysis*. Springer-Verlag New York.

Wood, S. N. (2017). *Generalized additive models: An introduction with R (2nd edition)*. Chapman and Hall/CRC. https://doi.org/10.1201/9781315370279

Wright, R. F., Couture, R. M., Christiansen, A. B., Guerrero, J. L., Kaste, Ø., & Barlaup, B. T. (2017). Effects of multiple stresses hydropower, acid deposition and climate change on water chemistry and salmon populations in the River Otra, Norway. *Science of the Total Environment*, *574*, 128–138. https://doi.org/10.1016/j.scitotenv.2016.09.044

Zięba, G., Staknas, S., Ives, M., Godard, M. J., Seymour, J., Carter, M. G., & Copp, G. H. (2014). Long-term decline of barbel *Barbus barbus* in the original course of the Lower River Lee (England), with particular reference to the survival of tagged fish during a water pollution incident. *Fundamental and Applied Limnology*, *185*(1), 43–53. https://doi.org/10.1127/fal/2014/0542

How to cite this article: Lennox, R. J., Thiemer, K., Vollset, K. W., Pulg, U., Stranzl, S., Nilsen, C. I., Haugen, T. O., & Velle, G. (2022). Behavioural response of brown trout (*Salmo trutta*) to total dissolved gas supersaturation in a regulated river. *Ecohydrology*, *15*(1), e2363. https://doi.org/10.1002/eco.2363